

European Organization for Nuclear Research

CERN AB Departement

CERN-AB-Note-2008-018

Simulation of Wire Scanner Heating by the Electromagnetic Field of a Particle Beam

T. Kroyer

Abstract

It was found in several machines that wire scanners may break due to beam-induced heating. In this paper the losses in the wire due to the fields of a passing particle beam are calculated using numerical simulation tools. Special care was taken when modeling the small diameter wire. The heating of carbon wires with LHC beam is calculated and the different regimes at low and high frequency are discussed.

Geneva, Switzerland
April 2008

1 Introduction

In the CERN LEP, SPS and other machines it was found that the carbon fibers used in wire scanners may break due to beam-induced heating [1, 2, 3]. A significant part of the heating is due to power from the electromagnetic field of the beam that is dissipated in the wire. For the LHC wire scanners this effect should be quantified. This is the goal of the simulations reported here. In this paper only the direct beam fields are considered. The fields in resonant structures can be damped using ferrites as shown e.g. in [1, 4].

2 Geometry

For the simulations Ansoft HFSS was used [5]. The geometry is shown in Fig. 1. The beam pipe with the wire scanner cavity was approximated by a square cross-section chamber. Trapped mode effects in the wire scanner cavity are supposed to be cared for by the addition of ferrites and not treated in this work. Here we consider only the effect of the direct electromagnetic fields of a passing beam. A wire simulation was done, i.e. the beam in the chamber is represented by a TEM transmission line, where the inner conductor radius corresponds to the rms beam size. The wire was modeled as being directly connected to the beam pipe. This is an approximation justified by the fact that the transmission line connected to the fork where the wire is fixed has a low impedance compared to the wire resistance of $\approx 2000\Omega$ and is terminated by a 50Ω resistance. A more accurate model including the fork and the wiring is of course possible but much more complex; The present model should be a reasonable but slightly pessimistic approximation.

In order to limit the number of mesh tetrahedrons the beam as well as the carbon wire were modeled by hexagonal cylinders. The hexagons are inscribed into the ideal circular elements, which makes the elements look a bit smaller ($\approx (1 - \sqrt{3}/2)/2 = 7\%$ smaller effective radius). For the wire conductivity the measured value of about $4e4$ S/m was used. The model parameters are summarized in the Table 1. Due to the very small wire

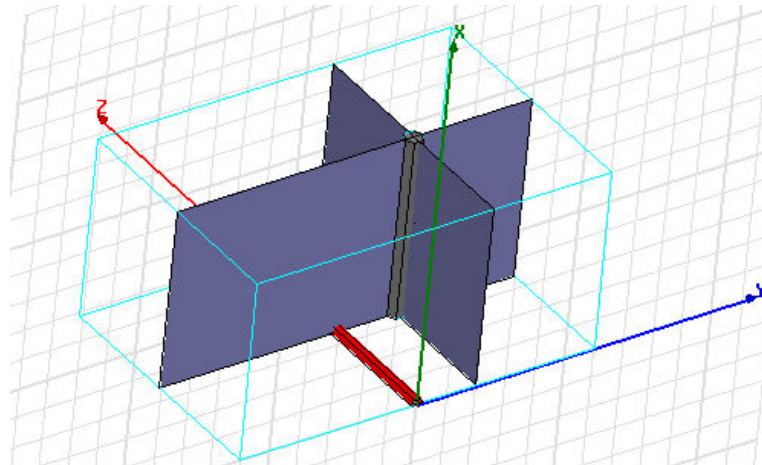


Figure 1: Geometry used for the simulation of the carbon wire heating. Only the upper half of the structure is modeled. The red wire represents the beam. The radius of the grey carbon wire is scaled up by a factor 100 here for clarity of display.

parameter	unit	value
beam pipe side length	mm	60
structure length	mm	40
rms beam size	mm	1
carbon wire radius	μm	15
carbon wire conductivity	S/m	4e4
carbon wire relative permittivity	1	1

Table 1: Parameters used in the simulation.

size special care had to be taken to get an acceptable convergence. The power lost in the wire was monitored as a function of the number of mesh refinement runs. It has the tendency to decrease for successively finer meshes. Up to 12 mesh iterations were used. Judging from the drop of the power over the last meshes the given results may overestimate the actual lost power roughly by 20%.

3 Results

3.1 Field pattern

The electric field in two cuts across the wire is shown in Fig. 2(a). Close to the beam the electric field is $\propto 1/r$, but there is a concentration around the carbon wire. The electric field of the beam drives a current along the wire, which is depicted in Fig. 2(b). The effect of the magnetic field is negligible, since it induces currents running parallel to the beam, which are not important in the thin wire. Please note that the current in the wire is zero on the beam axis and increases monotonically as one approaches the chamber wall. This behaviour can be explained by basic arguments.

It is assumed that the wire resistivity is large such that the E field is only slightly perturbed. For symmetry reasons the current must be zero at the beam axis. Going away from the beam axis the projection of the E field onto the wire increases. For not too high frequencies ($\lambda \ll \text{chamber radius}$) the E field can be considered in a quasistatic approach. The E field can be integrated along the wire to give a voltage between the wire center and a given point. Going towards the chamber this voltage and therefore the current must increase to reach its maximum at the beam pipe wall. The losses in the wire are proportional to the current squared. This qualitative picture is illustrated in Fig. 3.

3.2 Losses on the carbon wire

The losses on the wire scale with the square of the current density. They increase with the distance from the beam pipe center and with frequency (Fig. 4). The source data for different offsets o are attached:

- $o = 0 \text{ mm}$ 
- $o = 2 \text{ mm}$ 
- $o = 5 \text{ mm}$ 

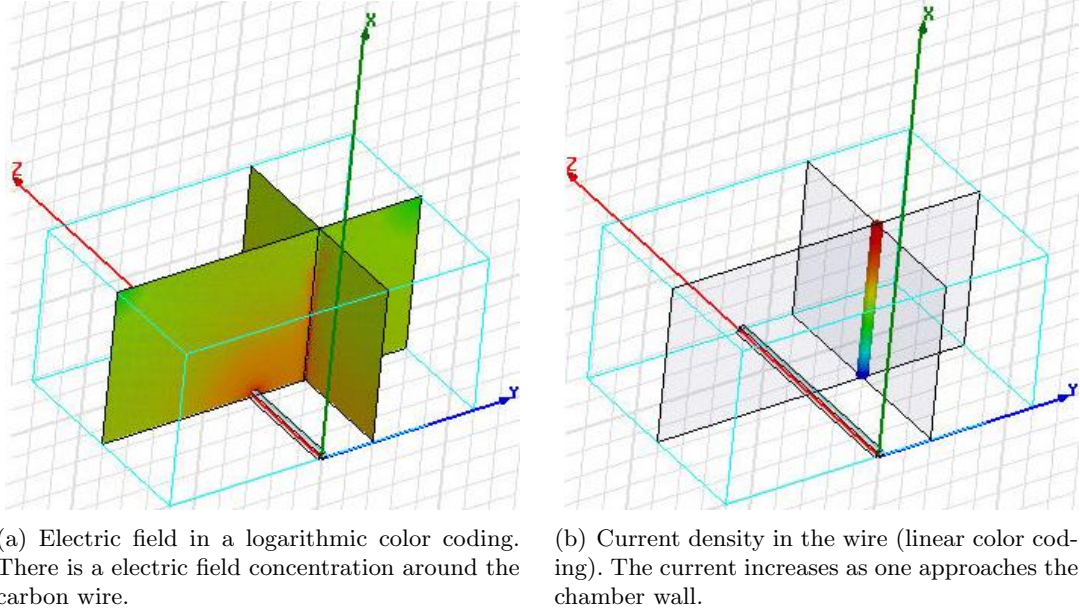


Figure 2: The fields in the simulated structure at 40 MHz, wire offset 10 mm.

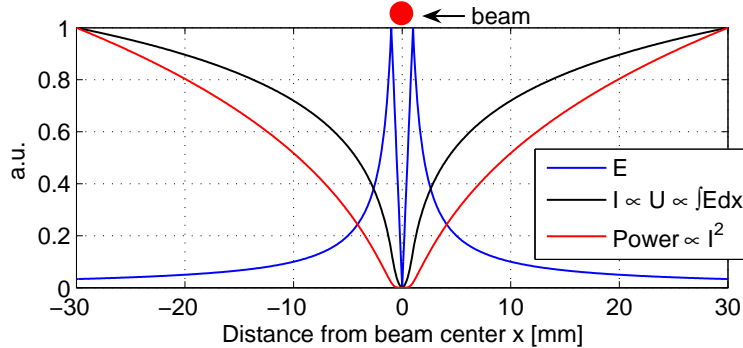


Figure 3: Qualitative picture of the beam's E field in a circular beam pipe. The losses in a weakly conducting wire should increase when going from the center towards the beam pipe.

- $o = 10$ mm
- $o = 20$ mm

The quantity given is the Volume loss density. To get the line loss density one has to multiply by the wire cross-section of $(15\mu\text{m} \cdot 0.93)^2\pi$, where the factor 0.93 is the correction for the hexagonal geometry. The total (beam) power incident on the waveguide port of the structure is normalized to 1 W.

The simulated data should be compared with measured from LEP. Fig. 5 shows digitized video recordings of an $8\ \mu\text{m}$ wire scanning a 0.8 mA beam. Successive traces are taken during one single scan. The little dip in the last trace represents the local heating by the direct beam impact. There is very good qualitative agreement between this measured data from LEP, the simple analytic approach (Fig. 3) and the simulated

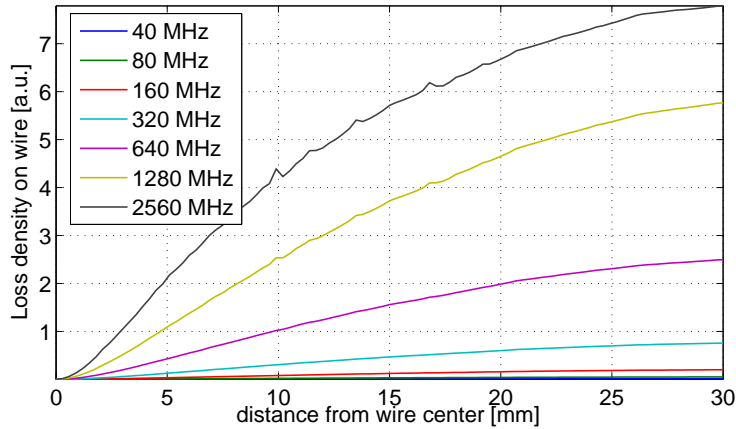


Figure 4: Losses on the wire as a function of the distance from the wire center for a wire offset of 2 mm.

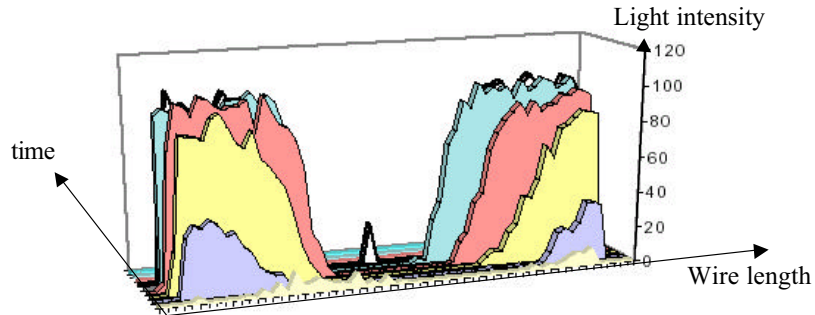


Figure 5: Optical observation of a LEP wire scanner. During a single scan the carbon fiber is set glowing, starting on the sides. The beam is in the center of the horizontal axis. Data of [2], taken from [3].

data for LHC (Fig. 4).

The total power dissipated on the carbon wire was evaluated by integrating the losses over the wire volume. The results for a scan in wire positions are shown in Fig. 6. The values given are the fraction of the total field power that is dissipated in the carbon wire.

Fig. 7 depicts the losses on the wire for two different wire conductivities. Two distinct regimes can be identified:

- In the low frequency regime the carbon wire couples inductively to the beam. The beam acts as a current source, which means that the losses are given by $P \propto I^2 R$, where I is the beam current and R the wire resistance. Since we have $R \propto \sigma^{-1}$ with the conductivity σ , the losses *decrease* for better conductivity. The skin effect is not important below several GHz since the wire radius is smaller than the skin depth. In addition, at low frequencies $P \propto f^2$, which can be easily derived from Maxwell's Equations neglecting the displacement currents.
- At higher frequencies the wire couples mainly capacitively and the effect of the beam can be visualized by a voltage source. Then $P \propto U^2/R$, where U is the

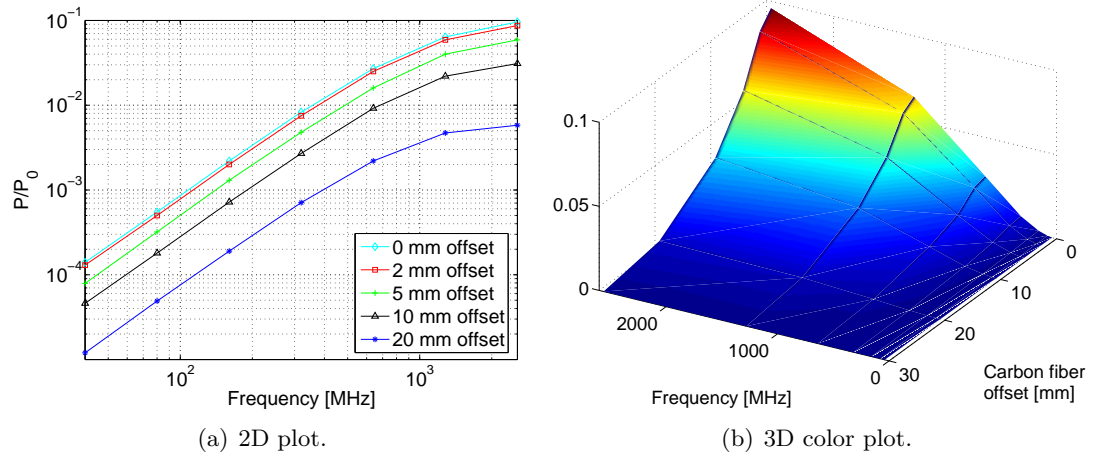


Figure 6: Total relative losses on the carbon wire for different wire offsets and frequencies.

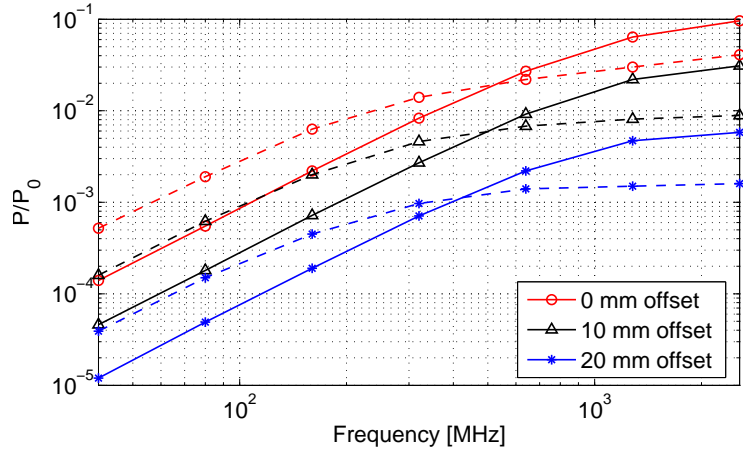


Figure 7: Total relative losses on the carbon wire for different conductivities. Solid traces: $\sigma = 4 \cdot 10^4 \text{ S/m}$, dashed traces: $\sigma = 1 \cdot 10^4 \text{ S/m}$.

beam potential. In this case $P \propto \sigma$, i.e. the losses *increase* for larger conductivity. A scan with different wire permittivities was also done, but it was found that the permittivity does not affect the losses on the wire. For a given beam the power deposited in the wire can be calculated by weighting the relative losses from Fig. 6(a) with the spectrum of the beam. The field power in the 40 MHz harmonics of nominal LHC beam at top energy is depicted in Fig. 8. The raw spectra are attached for nominal LHC beam at

- injection energy
- top energy

as a function of frequency [Hz], for Gaussian (second column) and \cos^2 (third column) longitudinal bunch profile. From experience with the SPS a Gaussian profile is believed

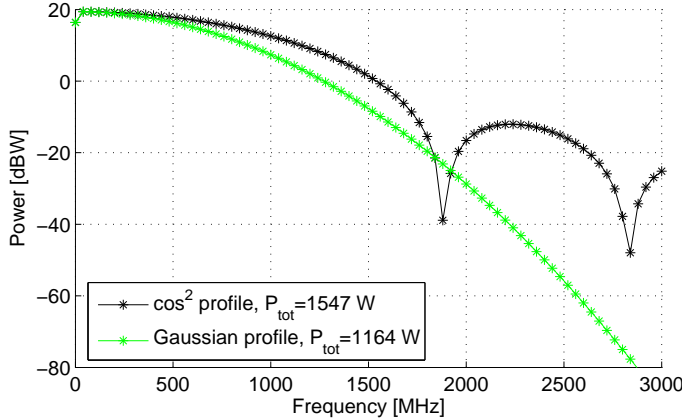


Figure 8: The power in the harmonics of nominal LHC beam at top energy, 4σ bunch length 1.06 ns.

to be more realistic.

For different beams the power in the beam field can be scaled as follows:

- It is proportional to the square of the instantaneous beam current, i.e. the bunch intensity.
- It scales linearly with the number of bunches. However, the spectrum looks very different for a single bunch compared to a full machine. In a full machine with 25 ns bunch spacing the spectrum consists exclusively of 40 MHz harmonics, while a single bunch spectrum is made up of multiples of the ≈ 11 kHz revolution frequency.
- The effect of the beam size is very small except when the wire is intercepting the beam. In this case for smaller beams there is more RF power deposited in the center of the wire. Integrated over an entire scan this should be negligible.

The resulting total losses as a function of wire offset are shown in Figs. 9.

Conclusion

The beam-induced heating of a carbon fiber used in LHC wire scanners was simulated. On account of the tiny fiber diameter the model had to be optimized to reach sufficiently good numerical convergence. The heating is due to resistive losses of the currents induced by the beam's electric field. The losses are small in the middle of the wire, they increase going towards the beam pipe. Scaling of the results for different beam types and intensities is possible.

Acknowledgements

I would like to thank F. Caspers and M. Sapinski for inspiring discussions.

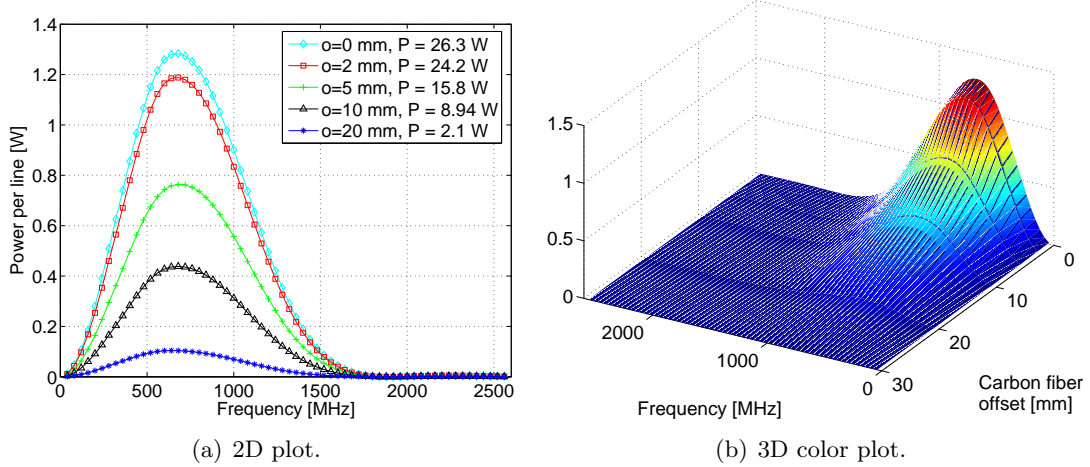


Figure 9: Total losses on the carbon wire for nominal LHC beam at top energy.

References

- [1] Roncarolo, F., Caspers, F., Dehning, B., Jensen, E., Koopman, J., Malo, J.F., *Cavity mode related wire breaking of the SPS Wire Scanners and loss measurements of wire materials*, PAC'03, Portland, USA, CERN-AB-2003-067-BDI (2003)
- [2] Fischer, C., Jung, R., Koopman, J., *Quartz wires versus carbon fibres for improved beam handling capacity of the LEP wire scanners*, CERN-SL-Div-Rep-96-009-BI, Geneva (1996)
- [3] Wittenburg, K., *Wire scanners*, http://adweb.desy.de/mpy/hera/BeamDynamicsMeeting/y04m01d08/KWittenburg_WireScanner.pdf (2004)
- [4] Kroyer, T., Caspers, F., *Wire Measurements on the LHC wire scanner* http://ab-abp-rlc.web.cern.ch/ab-abp-rlc/Meetings/2006/2006.02.17/wire_scanner_wire_measurements.pdf (2006)
- [5] www.ansoft.com